

Methods of Measurement and Strategies for Binder Removal in Ceramics

F. Raether* , A. Klimera*

* Fraunhofer ISC, Würzburg, Germany

received: 15.02.2008, revised: 10.07.2008, accepted: 30.07.2008

Keywords: binder removal, debinding, ceramics, kinetic field, thermal analysis

Abstract

Binder removal was investigated with various oxide and non-oxide ceramics and different binders. In situ measuring methods were used to obtain weight loss, dimensional changes, heat transfer and wetting properties and to identify evolved gas species during thermal debinding with conditions similar to production furnaces. In addition, gas permeation, strength and microstructure were investigated in partially debinded and quenched samples. A model free method was developed allowing prediction of debinding kinetics based on the experimental data. With small components weighing up to 100 g maximum safe rates were determined experimentally. Using the kinetic model considerable reductions in debinding times were obtained.

Introduction

During production of ceramics, organic additives such as binders, plasticizers and deflocculants have to be added to the inorganic raw materials, to achieve the required visco-elastic properties for forming and processing of the green parts. (In the following the organic additives are summarized as binder). After forming and before sintering, binder has to be completely removed, without affecting the microstructure of the inorganic components. During thermal debinding, binder usually is removed via the gas phase. The long chain binder molecules are thermally split or oxidized, producing CO₂ and H₂O if they degrade completely [1,2]. The gaseous reaction products have to reach the components surface via the pore channels. The flow resistance of the pore channels causes an overpressure inside the green bodies, when debinding is too fast, which can lead to cracks and fracture:

$$\frac{P_{centre}}{P_{surface}} = \left(1 + \frac{\mu \kappa R T}{M P_{surface}^2} L^2 r \right)^{1/2} \quad (1)$$

with P = gas pressure at centre respectively surface of the part, μ = viscosity of gas, κ = permeability, R = gas constant, T = absolute temperature, L = characteristic

half-length of part (e.g. its smallest radius), r = reaction rate, M = molar mass of gas species [1].

If the binder fills the pores completely, the diffusion of volatile components within the binder controls the transfer to the surface of the components. When the vapor pressure of the volatile components exceeds the external pressure, blisters are formed within the binder which can deteriorate the green part [3]. Usually extremely small heating rates are required to allow for a release of volatile species through the binder. The diffusion within the binder can also control debinding in green components where the pore channels are partially filled with gas. In that case, the size of clusters formed by binder and inorganic particles is critical for the distance which has to be covered via the slow process by the volatile species [3].

On the other hand, a slow debinding process is expensive in industrial production. Therefore, the fastest debinding cycle has to be identified, which can be realized without risking any damage at the components. This task is made more difficult due to the fact that the reaction rates depend on the partial pressure of the reaction products. In addition permeation and diffusion of the gaseous molecules in the pore channels change with temperature as well as with debinding rate. An increasing degree of debinding, raises the binder free pore volume. Therefore, permeability and effective diffusion coefficient of gases in the pore channels increase as well. Further aspects for the optimization of debinding cycles come from the interac-

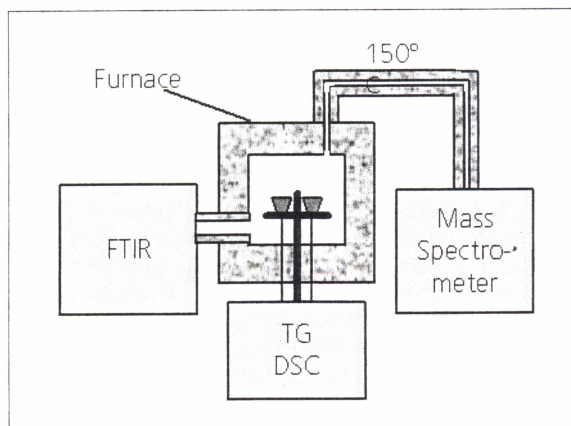


Fig. 1 Principle scheme of the TG-DSC-FTIR-MS device

Corresponding author: Friedrich Raether, Fraunhofer ISC, Neunerplatz 2, D-97084 Würzburg, Germany, Phone: 00 49 (0) 931 4100 200, Fax: 0049 (0) 931 4100 299, E-mail: friedrich.raether@isc.fraunhofer.de

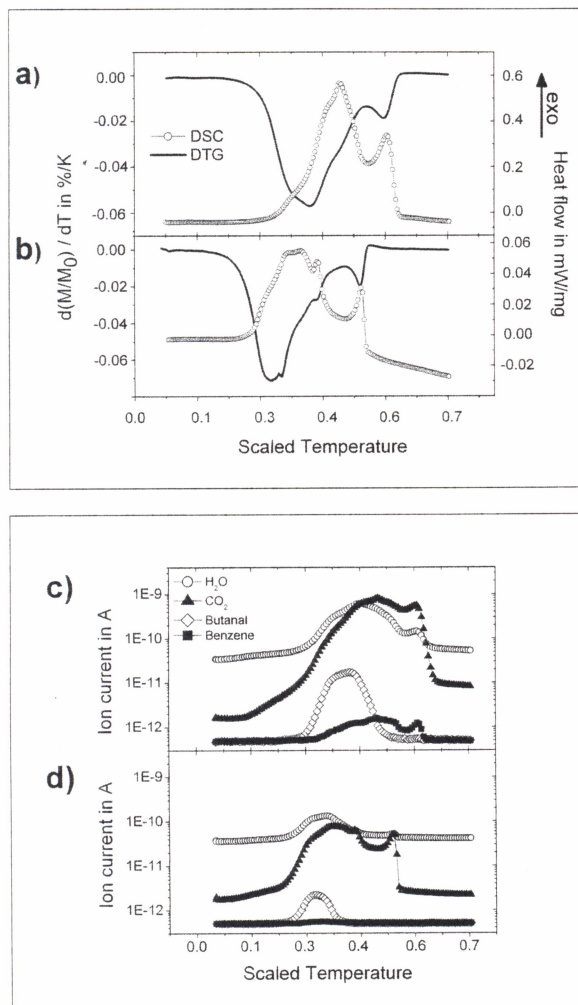


Fig. 2 Debinding of PZT green parts: Differential Thermogravimetry (DTG) and Differential Scanning Calorimetry (DSC) at a heating rate of 5 K/min [a] and 0,5 K/min [b] as well as intensity of the mass spectrometric signals of different gas species at a heating rate of 5 K/min [c] and 0,5 K/min [d]

tion of the residual binder with the inorganic particles. Thus, usually strength is decreasing during binder burnout, i.e. with proceeding degree of debinding, the acceptable overpressure is decreasing. Further interactions during debinding can appear with thermoplastic binders, because capillary forces can cause a redistribution of the ceramic particles and redistribution of the viscous binder in the pore network. Forming processes like cold isostatic or uniaxial pressing only demand a small binder fraction (< 2,5 %). Thus debinding is relatively unproblematic. To produce larger components and components of more complex shape, forming processes like tape casting and injection molding are increasingly applied. For that purpose, large fractions of binder in the green parts are requested. This causes massive problems during debinding, mainly in large components. Regarding non-oxide ceramics, such as AlN, SiC, BN, MoSi₂ or TiC, debinding creates additional problems, because it has to be performed without oxygen in an inert atmosphere. During pyrolysis in inert atmosphere non-volatile, elemental carbon occurs, which remains in the components. This residual carbon may affect sintering and the final quality of the components, e.g., it causes discoloration, density gradients and warpage. It is assumed that the intermediate for-

mation of aromatic hydrocarbons by the reaction of decomposition from the pyrolysis of the used aliphatic binders is responsible for the formation of elementary carbon [4].

Temperature gradients inside the green parts also play an important role for larger components respectively higher heating rates. A coupled simulation of temperature distribution, reaction rates and gas permeation was performed using Finite Element methods. Using this method, the dehydration reactions occurring during firing of high voltage insulators were considered in the optimization of the heating cycle [5]. In principle the binder removal can be optimized in a similar way. But considering the complexity of the related phenomena, many material data are required which are difficult to obtain. Therefore, simplified and more efficient models are to be preferred.

The present paper summarizes recent investigations [6], [7] on debinding of oxide and non-oxide ceramics, where various ceramic systems (PZT, AlN, SiC, MoSi₂ as well as a mixed oxide ceramics), and binders – based on polyvinyl butyral (PVB), polyvinyl alcohol (PVA) polyethylene glycol and wax emulsion – were included. At first, measuring methods are presented, which were essential for a description of debinding phenomena. Subsequently, strategies for the development of efficient debinding cycles are discussed.

Results and Discussion

The most important measuring method for investigation of binder burnout was Thermogravimetry (TG). By means of the weight loss, the degree of debinding was determined in situ very accurately after buoyancy effects have been corrected. Reproducibility was improved by conditioning of the green parts (previous storage at defined humidity and temperature) and maintaining constant sample dimensions. Small samples (approx. 100 mg) were analyzed with a customary Thermobalance (Netzsch STA 449c, Selb, Germany). Thereby, the heat of reaction was measured simultaneously. This was done qualitatively by differential thermal analysis (DTA) or quantitatively by Differential Scanning Calorimetry (DSC) in comparison to an inert reference sample. In addition, the evolved gas species during debinding were detected, using infrared spectroscopic methods FTIR (Bruker Tensor 27, Ettlingen, Germany) as well as mass spectroscopy (MS, Netzsch QMS 403 C, Selb, Germany) (Fig. 1). MS and FTIR methods provided additional information regarding the evolved gas species, for molecules without dipole moment were not IR active and molecules with equal ratio of ion charge to mass (e.g. CO₂ and N₂) could not be distinguished by MS. Exemplarily, measurements of PZT green parts produced by tape casting with a PVB based binder are shown in Fig. 2. Reaction rates changed considerably when the heating rates were varied, e.g., at the lower heating rate of 0,5 K/min, no aromatic hydrocarbons (benzene) were detected whereas a distinct benzene MS signal was obtained at 5 K/min. This was attributed to the lower partial pressure of hydrocarbons for the lower heating rate that decreases the reaction rate. Thus conclusions about reaction order could be obtained. More details on these measurements were given in [6].

Larger samples with approx. 100 g weight were measured with a special Thermo-Optical Measuring device

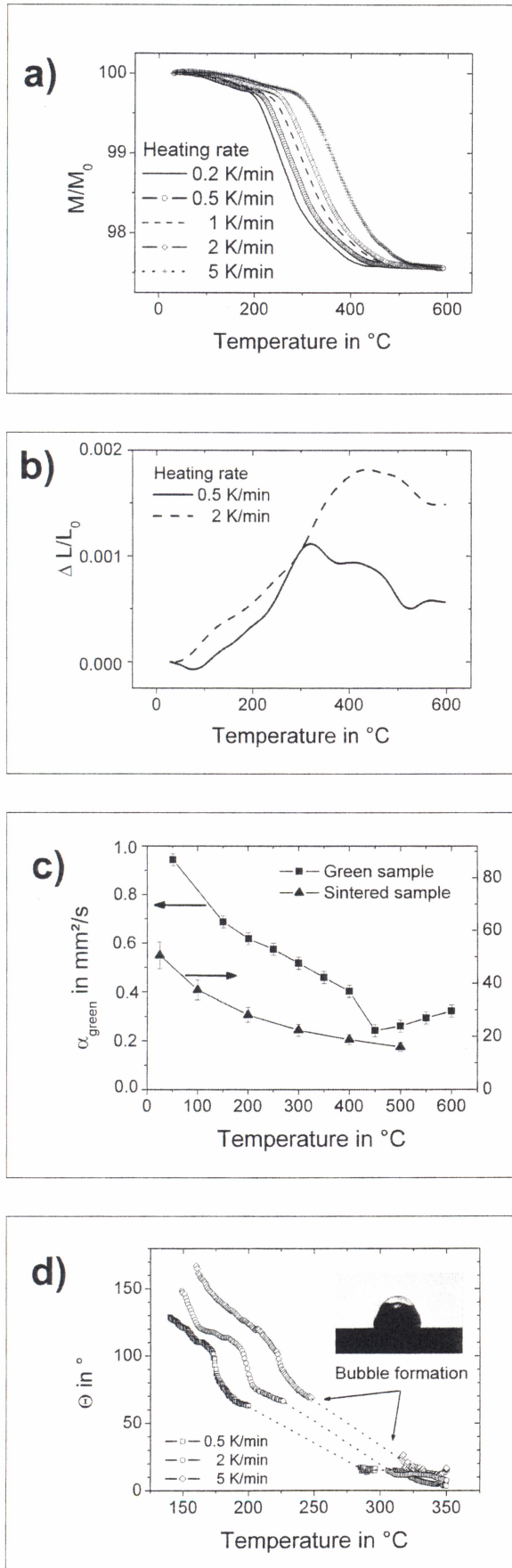


Fig. 3 In situ measuring data during debinding of AlN, measured using TOM: Loss of weight at variable heating rates [a], change of lengths [b], thermal diffusivity at a heating rate of 2 K/min [c] and wetting angle between binder and dense AlN substrate [d]. (All measurements were performed in nitrogen.)

(TOM) [8]. The device had a weight sensor, from which the specimen holder was suspended. Weight changes were recorded by the shift of natural vibrations of a string that was included in the system. Simultaneously, dimensional changes of the sample during binder burnout were detected by an optical method recording the profile of the sample by a CMOS camera and a telecentric optic during back light illumination with a diffuse light source. Crack formation during binder burnout was detected by sudden dimensional changes or by sudden weight changes. The atmospheres in various industrial furnaces were reproduced by different natures of heating element ($MoSi_2$ and graphite) and insulating materials (e.g., alumina or carbon fiber board). Thus, binder burnout in air as well as in inert and reducing atmosphere or in atmosphere containing water vapor was investigated. The latter reproduced the conditions in gas-fired furnaces [5]. Binder burnout experiments were also performed in closed crucibles which were suspended to the weight sensors. This was considered important, if industrial debinding processes with a high organic volume compared to the furnace volume were to be reproduced.

By means of a laser-flash add on to TOM [8], thermal diffusivity was determined during binder burnout. The thermal diffusivity is required to calculate temperature gradients, which can be relevant during heating of large components. In addition, the effect of temperature gradients within the setup was investigated using a large granitic cube as sample support. During constant rate heating the large heat capacity led to a temperature lag of the support compared to the sample.

It was shown that with thermoplastic binders, very high heating rates could be used without damaging the samples. That suggests, that thermal stresses were not relevant in the debinding stage when some plasticity of the parts was provided by the binder.

Wetting between the different binders and the ceramics has been investigated also by TOM. For that, a small portion of the binder was deposited on a dense substrate of the respective ceramics and heated with a constant heating rate [9]. The contact angle was determined from the profile of the droplet which formed during heating. Fig. 3 shows weight loss, changes of dimensions, thermal diffusivity and wetting angle, measured during debinding of dry pressed AlN green parts. Weight loss started at 100 °C and was enhanced between 200 °C and 500 °C. Higher heating rates shifted the weight loss curves to higher temperatures (Fig. 3a). During debinding a small expansion was measured (Fig. 3b). Thermal expansion had been corrected by scaling the data with the length of an already debinded sample measured at the respective temperatures. Thermal diffusivity stronger decreased during debinding compared to that of a sintered AlN sample, measured in the same temperature range (Fig. 3c). This was attributed to the removal of the binder at the particle contacts and the corresponding increase of thermal resistance. The wetting angle was initially larger than 90°, i.e. the binder was non-wetting (Fig. 3d). This could explain the expansion of the samples during debinding (see Fig. 3b) since a non-wetting liquid between the particles is well known to cause swelling of compacts [10]. At temperatures between 180 °C and 240 °C, the wetting angle decreased below 90°. In this temperature range the

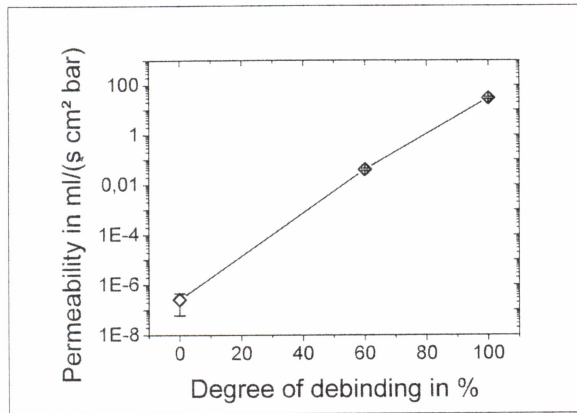


Fig. 4 Permeability of nitrogen through partially debinded and quenched PZT layer of 0,5 mm thickness measured at ambient temperature

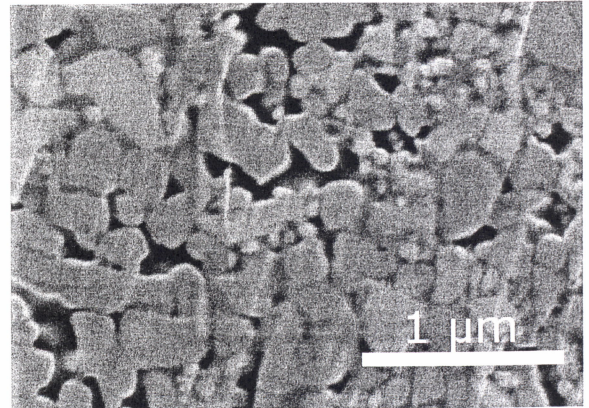


Fig. 6 SEM image of a partially debinded green part of mixed oxide ceramic showing ceramic particles, binders and pores

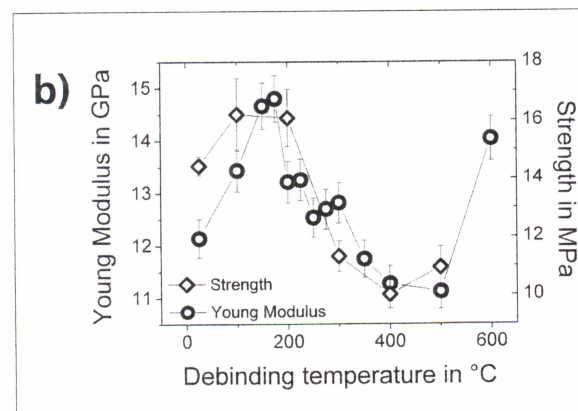
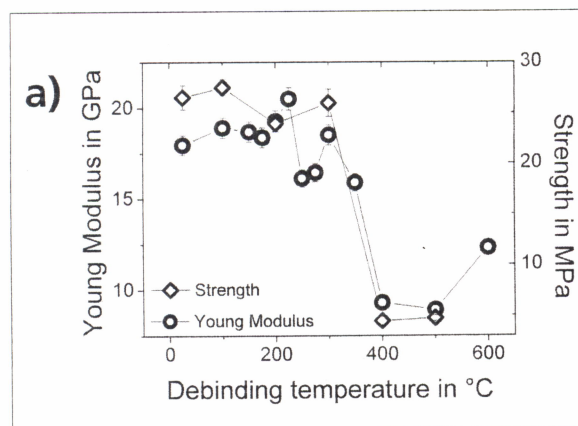


Fig. 5 Strength and Young's modulus for partially debinded green parts made of mixed oxide ceramic [a] and MoSi₂ ceramic [b]

maximal weight loss rates were detected. Between 200°C and 330°C gaseous blisters were formed in the binder, so that no measurement of the wetting angle was possible. This temperature region was considered especially critical due to possible damage if the blistering occurred in clusters filled with binder within the porous compacts.

Permeation and diffusion of gas species through partially debinded samples were measured by pressing disk samples between two metal sheets with concentric holes in a gas tight environment. Starting from different pure gases or vacuum on both sides of the sample, the change of partial pressure was measured versus time according to the Wicke Kallenbach

method [11]. From the data, permeabilities and coefficients for interdiffusion were fitted. These measurements were performed at temperatures up to 300°C but it was very tedious to avoid leakages at the surface of the rather fragile samples. Fig. 4 shows the large change of permeability by seven orders of magnitude measured during debinding of a tape cast PZT green sample.

Strength was measured at room temperature by the ball on ring method using disk shaped, partially debinded samples (Fig. 5) [7]. In addition, Young's modulus was determined by means of ultrasonic measurements. As a rule, Young's modulus decreased with degree of debinding. For some binder systems, an initial increase of Young's modulus was detected after partial debinding (Fig. 5b). This was attributed to a thermal curing of the respective binder. A close correlation between Young's modulus and strength at all investigated samples was observed. As no absolute value of strength was needed, the time-consuming measurements of strength were substituted by measurements of Young's modulus. The Young's modulus can also be determined in situ during debinding to further reduce the experimental effort [12].

The microscopic distribution of the binder in the green parts was investigated in the scanning electron microscope (SEM, Zeiss Ultra, Oberkochen, Germany) using polished sections. Polished sections were prepared by ion beam etching using 6 keV Ar ions by the so-called Cross Section Polishing method (CSP, Jeol SM-09010, Tokyo, Japan). The extremely small angle of ion incidence prevented a selective etching of the binder. Fig. 6 shows a SEM image of binder (dark-grey), ceramic particles (light grey) and pores (black) in a partially debinded pressed green part made of a mixed oxide ceramic (Al₂O₃-TiC/N-ZrO₂).

Modeling Debinding Kinetics

The kinetics of binder burnout was determined according to the so-called Kinetic Field method. For that, the degree of debinding was measured by means of TG using different constant heating rates (compare Fig. 3a). The corresponding weight loss rate was plotted logarithmically versus the inverse absolute temperature in an Arrhenius type diagram (Fig. 7). The method has been successfully employed for the description of sintering shrinkage since the early nineties [13, 14]. It is similar to a method proposed

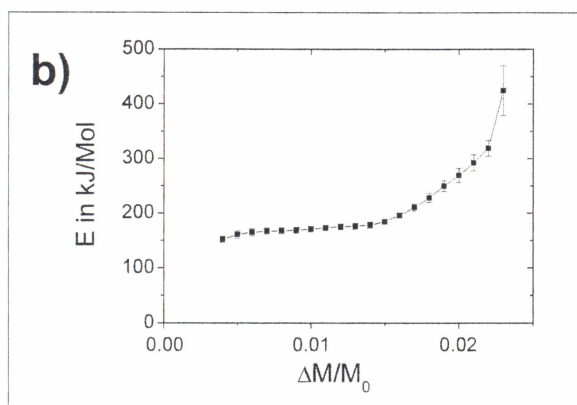
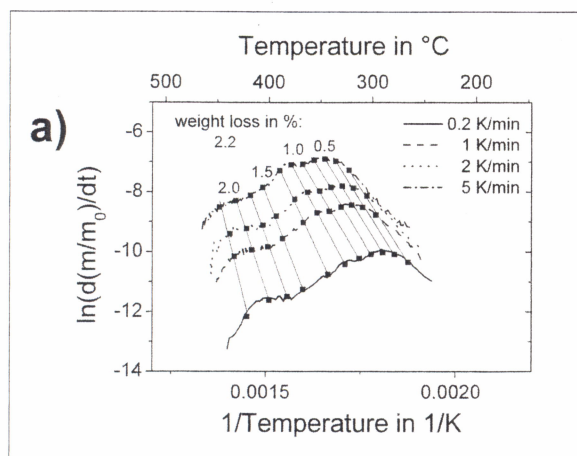


Fig. 7 Debinding of AlN green parts: Kinetic Field with iso-weight loss lines [a] and activation energies determined from their slope [b]

recently which uses a master curve for the description of the binder removal kinetics [15]. First, the weight loss rates increased with temperature, then passed a maximum at about 300°C and finally declined to very small values, when binder burnout was finished. At higher heating rates, the weight loss rate was because debinding was going on faster (Fig. 7). On the curves corresponding to the different heating rates, points belonging to the same weight loss were connected. They formed one iso-weight loss line respectively. The iso-weight loss lines could be fitted by polynomials of second order with all debinding processes. Mostly even first order polynomials, i.e. straight lines could be used. From the slope m of the iso weight loss lines, an apparent activation energy E_{Act} was formally derived according to: $m = -E_{Act}/R$ (with R = gas constant, Fig. 7b). For aluminum nitride with PVB binder this apparent activation energy was 180 kJ/Mol up to a weight loss of 1,5 % (Fig. 7b), which is in agreement to previous investigations [16]. This weight loss was attributed to the separation of side-chains. Afterwards an increase in activation energy was found (Fig. 7b) which indicated a change in the rate controlling mechanism that was explained by the degradation of cross linked and cyclic structures [9].

More importantly, the set of iso-weight loss lines was used to predict the debinding rate for arbitrary debinding cycles. For a given degree of debinding M/M_0 (e.g. a weight loss of 1 % in Fig. 7a) at time t and temperature T , the corresponding point was identified in the Kinetic Field diagram. The respective weight

loss rate $d(M/M_0)/dt$ was read off at the ordinate. It determined the degree of debinding at time $t+\Delta t$, whereas the new temperature was calculated from the given heating rate α during the respective time interval Δt :

$$\begin{aligned} M/M_0(t+\Delta t) &= M/M_0(t) + d(M/M_0)/dt \cdot \Delta t \\ T(t+\Delta t) &= T + \alpha \cdot \Delta t \end{aligned} \quad (2)$$

So the next point was identified in the Kinetic Field diagram. By successive calculation of the path integral, the corresponding weight loss M/M_0 could be determined using equation (2) for arbitrary time-temperature cycles. The reverse process was also possible by specially designed software: Using given weight loss rates the corresponding time-temperature cycles were calculated by the computer. The Kinetic Field method didn't need any microscopic model which was considered essential considering the complexity of microstructural changes.

Despite this simplification, an appropriate description of the debinding kinetics for all green parts investigated was obtained. In contrast to the master curve approach [15], the Kinetic Field method may consider a change of activation energy during debinding. Many binder systems required this enhanced flexibility (compare Fig. 7b). It is pointed out that the successful transfer of the results to production furnaces relies on measuring with similar sample dimensions and furnace atmospheres. Whereas the first can be solved using special weight sensors the later usually leads to debinding in closed crucibles. By that, sufficiently high partial pressures of volatile organics were obtained in the vicinity of the sample. So production

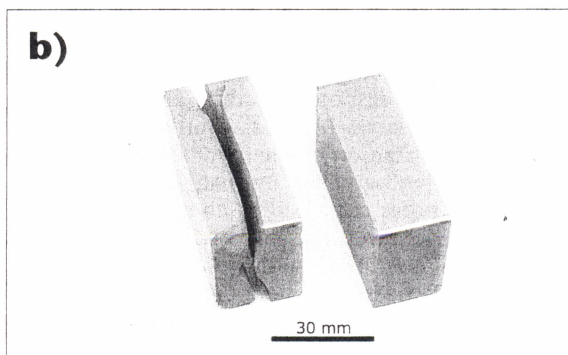
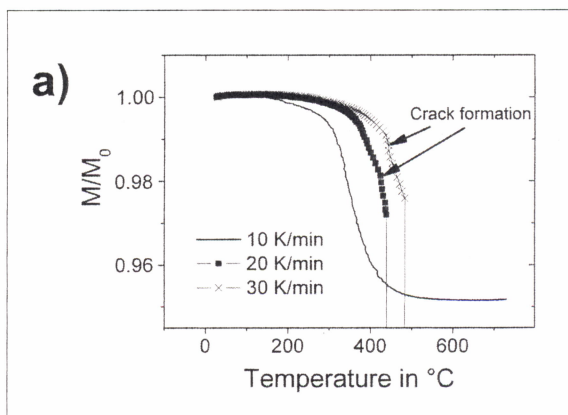


Fig. 8 Determination of the maximum safe rate for SiC-green parts: TG measurements at variable heating rates [a] and destroyed and defect free samples after debinding [b]

furnaces with a large ratio of parts volume to furnace volume could be reproduced more realistically.

Optimization of Debinding Processes

The knowledge of the debinding kinetics was used to optimize the debinding process. So the maximum safe weight loss rate was determined, when the green parts were just not damaged. For that, debinding was measured with TOM on samples having a weight between 10 g and 200 g at much higher heating rates as used in production. Damaging was recognized from sudden changes in dimensions and weight of the samples (Fig. 8). The corresponding weight loss rate was multiplied by a safety factor (<1) and then used as maximum safe rate. Using the Kinetic Field, an optimized time-temperature cycle was calculated which exactly followed this rate during the entire debinding process. A similar approach was used for the debinding of multilayer capacitors, but instead of the Kinetic Field method, a feedback control of the furnace temperature by the measured weight loss rate had been installed [17]. The Kinetic Field method was considered superior to the feed back control because the later led to problems with temperature control and could not easily be transferred to other weight loss rates. The maximum safe rate could be increased during debinding when an increasing permeability led to a decrease of overpressure. Vice versa, it was decreased to consider decreasing strength. If the geometry of the parts was changed, especially its characteristic length, the maximum safe rates had to be adjusted (compare equation 1). Recently Lombardo has shown that a general relation between the maximum safe rate and the component size could not be derived from modeling debinding [18]. Therefore, it is suggested to repeat the experimental determination of the maximum safe rate with the respective components.

An alternative route to obtain the maximum safe rate was provided when a debinding process was already introduced in production. The respective time-temperature cycle was analyzed in the kinetic field and its maximum weight loss rate was identified as the maximum safe rate. Then the time-temperature cycle was shortened by increasing the weight loss rate in the other heating segments to the level of the maximum safe rate. Time savings of more than 30 % could be obtained by this method. Additionally, precautions considering critical gas formation by other mechanisms - not included in the maximum safe rate - were considered by adaptations of the heating cycle. E.g., the evaporation of volatile binder components or moisture at low temperatures and the blister formation at higher temperatures required smaller heating rates in the respective temperature segments. Using thermoplastic binders, capillary forces can lead to a redistribution of the binder at temperatures above the softening point. By that, larger clusters of neighboring pores can be filled completely with the binder whereas surrounding pores are depleted. (Segregation of a melt phase within porous powder compacts was investigated in more detail with respect to liquid-phase sintering [19].) If the binder has non-wetting properties (compare the low temperature region of Fig. 3d), thermodynamic driving forces can even lead to exudation of the binder. It was concluded, that higher heating rates in the respective temper-

ature segments can be useful to avoid segregation phenomena.

Summary and Outlook

For investigating thermal debinding, in situ measuring methods are available, making it possible to obtain relevant material data under conditions which are close to the conditions in production furnaces. The in situ methods are supplemented by permeation measurements and microstructural analyses, providing additional information on partially debinded and quenched samples. Maximum safe weight loss rates were identified empirically. The Kinetic Field method was used to predict debinding cycles according to the respective maximum safe rate. Existing debinding processes duration could be reduced considerably by this method. They were adapted to additional requirements resulting from processes accompanying binder burn out.

Acknowledgement

Companies CeramTec, ANCerem, Kennametal, FCT und GFE, participating in that projects are acknowledged for the supply of green parts and for valuable discussions. The German ministry of education and research (BMBF) and the Bavarian ministry of economics (BStmWiVT) are also acknowledged for funding of the projects [6], [7].

Literature

- [1] Shende R.V., Lombardo, S.J.: Determination of Binder Decomposition Kinetics for Specifying Heating Parameters in Binder Burnout Cycles, *J. Am. Ceram. Soc.* **85** (2002) 780-786
- [2] Lewis, J. A.: Binder Removal from Ceramics, *Annu. Rev. Mater. Sci.* **27** (1997) 147-173
- [3] Calvert, P., Cima, M.: Theoretical Models for Binder Burnout; *J. Am. Ceram. Soc.* **73** (1990) 575 – 579
- [4] Ferrato M., Chartier T., Baumard J.F. und Coudamy G.: Der Bindemittelabgang in keramischen Scherben, *cfi/Ber. DKG* **71** (1994), 8-12
- [5] Raether, F., Klimera, A., Baber, J.: In situ Measurement and Simulation of Temperature and Stress Gradients during Sintering of Large Ceramic Components. *Ceramics International* **34** (2008) 385-389
- [6] Optimierung von piezokeramischen Vielschichtaktoren für dynamische Anwendungen, Förderprogramm WING des BMBF, Förderkennzeichen: 03X2501B, 01.04.2004 – 31.03.2007
- [7] THENOX: Thermische Entbinderungstechnik für die Herstellung großvolumiger Bauteile aus Nichtoxidkeramik, Programm Neue Werkstoffe in Bayern, Förderkennzeichen: 0A447200504; 01.08.04 – 31.10.07
- [8] Baber, J., Klimera, A., Raether, F.: In situ measurement of dimensional changes and temperature fields during sintering with a novel thermo-optical measuring device, *J. Eur. Ceramic Soc.*, **27** (2007) 701-705
- [9] Klimera, A., Raether, F., Schulze Horn, P.: In situ Investigation of debinding of non-oxide ceramic. *Advances in Science and Technology*, **45** (2006) 1684-1689
- [10] German, R.M.: Sintering – theory and practice. John Wiley, New York (1996)
- [11] Wicke, E., Kallenbach, R.: Die Oberflächendiffusion von Kohlendioxid in aktiven Kohlen. *Kolloid-Zeitschrift*, **97** (1941) 135 - 151
- [12] Roebben, G., Bollen, B., Brebels, A., Van Humbeeck, J., Van der Biest, O.: Impulse excitation apparatus to measure resonant frequencies, elastic moduli, and internal friction at room and high temperature, *Rev. Sci. Instrum.* **68** (1997) 4511– 4515

- [13] Palmour H (1989) Rate-controlled sintering for ceramics and selected powder metals. In: Uskokovic D, Palmour H, Spriggs RM (eds) *Science of Sintering*, Plenum Press, New York, p 37
- [14] Zimmer, J., Raether, F., Jaenicke-Rößler, K., Leitner, G.: A system for rate controlled sintering by kinetic field approach. Proc. 9th Cimtec-World Ceramics Congress, Ceramics: Getting into the 2000's - Part B, Techna Srl (1999) 693-702
- [15] Aggarwal, G., Park, S.-J., Smid, I. and German, R.M.: Master Decomposition Curve for Binders Used in Powder; *Met. a. Mat. Trans. A*, 38A (2007) 606 -614
- [16] Liau, L., Peters, B., Krueger, D.S., Gordon, A., Viswanath, D.S., Lombardo, S. J.: Role of length scale on pressure increase and yield of poly (vinyl butyral)-barium titanate – platinum multilayer ceramic capacitors during binder burnout. *J. Am. Ceram. Soc.* **83** (2000) 2645 - 53
- [17] Verweij, H. and Bruggink, W. H. M.: Reaction-Controlled Binder Burnout of Ceramic Multilayer Capacitors; *J. Am. Ceram. SOC.*, **73** (1990) 226-31
- [18] Yun, J. W., Lombardo, S.J.: Effect of decomposition kinetics and failure criteria on binder-removal cycles from three-dimensional porous green bodies. *J. Am. Ceram. Soc.*, **89** (2006) 176 - 183
- [19] Shaw, T.M.: Liquid Redistribution during Liquid-Phase Sintering, *J. Am. Ceram. Soc.*, **69** (1986) 27-34